An Aperture-Shared High-Isolated MIMO Antenna Design Using Quarter-Wavelength Monopole as Differential-Mode Antenna

Mingjie Ma, Yu Li, Cuixia Huang, and Jiangwei Sui, *Member, IEEE*

***Abstract*—An aperture-shared high-isolated multiple-input–multiple-output (MIMO) antenna design is proposed in this letter for mobile terminals. A 1/4λ monopole antenna is utilized as the differential-mode antenna to avoid using the complex balanced-feeding structures, while a 1/2λ loop antenna is adopted as the common-mode one. Different from the existing differential-common modes MIMO antenna designs, the differential-mode antenna in the proposed design is of 1/4λ, and the geometrical asymmetry is exploited to compensate for the current asymmetry. Moreover, lumped elements are loaded at the end of antennas to miniaturize the antenna size, and a transmission-line model is presented to analyze the miniaturization principle. For validation, a self-decoupled MIMO antenna design working from 3.4 GHz to 3.6 GHz is presented using the proposed scheme. Results show that the isolation between the antenna pair is better than 21.7 dB, and the envelope correlation coefficient is lower than 0.002 across the working band with only a $0.1\lambda_0$ size.**

***Index Terms*—Antenna decoupling, mobile terminals, multiple-input–multiple-output (MIMO), mutual coupling, self-decoupling.**

I. Introduction

MULTIPLE-input–multiple-output (MIMO) technology serves as a fundamental enabler in fifth-generation (5G) mobile terminals to achieve spatial diversity and multiplexing [1]. However, the progressive evolution of mobile terminals has resulted in continually shrinking spaces for MIMO antennas, generating severe mutual coupling effects between antennas [2]. To resolve the antenna mutual coupling in mobile terminals, numerous decoupling methods have been proposed, where miniaturization is a critical point to be considered.

A straightforward idea for antenna decoupling is introducing decoupling structures between antenna elements to block or mitigate the original coupling, including neutralization line (NL) [3], [4], [5], defected ground structure (DGS) [6], [7], parasitic element [8], [9], decoupling network [10], [11], [12], [13], decoupling capacitor [14], [15], [16], and so on. However, these solutions inherently contradict terminal antenna miniaturization, and the physical connections in certain configurations substantially compromise design flexibility.

Another category is the self-decoupling scheme, which is free from using any external decoupling structure, so the volume of MIMO antenna arrays could be more compact. First, the self-decoupling effect can be directly realized by tactically manipulating the antenna geometry, such as asymmetric mirroring [17], [18], using the shared branch [19], and optimizing radiating branches [20], [21], [22]. In addition, the mutual coupling can also be self-mitigated by exploiting the orthogonality [23], [24], [25]; as well as mode decomposition [26], [27], [28], [29] of the antennas. A recent advancement employs orthogonality through differential/common mode antenna pairs to obtain excellent self-decoupling in a limited space [30], [31], [32], [33], [34]. The operational cornerstone resides in the differential-mode radiators, and the existing designs predominantly utilize 1/2λ resonant configurations to realize such differential-mode antennas with symmetrical and in-phase current distributions. Furthermore, the requisite balanced feeding mechanisms introduce substantial implementation complexity and associated cost escalation.

In this letter, the concept of using a 1/4λ monopole antenna as the differential-mode antenna is proposed to design a self-decoupled MIMO antenna pair. Since the 1/4λ monopole antenna possesses an asymmetrical in-phase current distribution, it is designed to be asymmetrically placed with a traditional common-mode loop antenna to compensate for the current asymmetry, so an asymmetric mode-orthogonal self-decoupling is successfully achieved. Furthermore, lumped elements are proposed to be loaded at the antenna ends to further minimize the antenna size. Compared with the existing self-decoupling methods using differential-common-mode methods, the proposed concept has two unique advantages.

1) The proposed MIMO antenna does not require balanced-feeding structures, which is convenient for printed circuit board (PCB) and antenna integration in mobile terminals.
2) Thanks to the 1/4λ differential-mode antenna and lumped element loading, the proposed MIMO antenna possesses a much smaller size, which is attractive for antenna miniaturization in mobile terminals.

II. Working Mechanism

First, the decoupling mechanism is illustrated in Fig. 1. Fig. 1(a) presents the current distribution of a typical inverted 1/4λ monopole antenna, where the terminal end is also bent for

Received 10 August 2025; revised 22 August 2025; accepted 5 September 2025. Date of publication 17 September 2025; date of current version 18 December 2025. This work was supported in part by the National Natural Science Foundation of China under Grant 62201625; in part by Guangdong Basic and Applied Basic Research Foundation under Grant 2025A1515010696; and in part by the Science, Technology and Innovation Commission of Shenzhen Municipality under Grant KJZD20240903101314019. *(Corresponding author: Jiangwei Sui.)*

Mingjie Ma, Yu Li, and Jiangwei Sui are with the School of Electronics and Communication Engineering, Sun Yat-sen University, Shenzhen 510275, China (e-mail: mamj25@mail2.sysu.edu.cn; liyu236@mail2.sysu.edu.cn; suijw@mail.sysu.edu.cn).

Cuixia Huang is with the School of Electronics and Communication Engineering, Sun Yat-sen University, Shenzhen 510275, China, and also with Lianzhou International Company, Ltd., Shenzhen 518000, China (e-mail: huangcx7@mail2.sysu.edu.cn).

Digital Object Identifier 10.1109/LAWP.2025.3610947

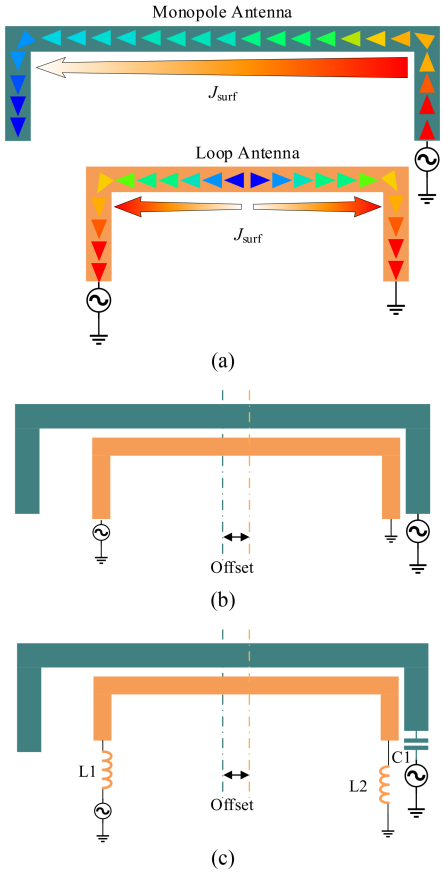

Fig. 1. Schematic description of the proposed self-decoupling concept. (a) Current distributions of a 1/4λ monopole antenna and a 1/2λ loop antenna. (b) Antenna geometry with asymmetrical arrangement. (c) Proposed antenna with asymmetrical arrangement and lumped elements.

size miniaturization, and the notation J_{surf} means the surface current density. It is well known that this type of monopole is a 1/4λ mode antenna, and its current distribution is in-phase throughout the whole branch.

On the other hand, there are two obvious features of the current distribution of the differential-mode antennas in the previous works: in-phase and symmetrical [30], [31], [32], [33], [34]. For the proposed inverted 1/4λ monopole antenna, the current reaches a maximum near the feeding arm and approaches a minimum at the open end. Although this distribution is not symmetrical like the classical dipole antenna, its in-phase characteristic may still be utilized to obtain a quasi-differential-mode antenna to achieve self-decoupling.

Meanwhile, a loop antenna is adopted as the common-mode antenna, as also shown in Fig. 1(a), which presents a typical common-mode distribution with maximum at the two ends and minimum at the middle point. Fig. 1(b) depicts the integrated geometry of the final design. It is observed that to enhance the self-decoupling performance, the inverted monopole and the loop antennas are placed with an offset to compensate for the current asymmetry by exploiting geometric asymmetry.

Besides, to satisfy the antenna miniaturization requirement in mobile terminals, the lumped elements are loaded at the proposed antennas to reduce the whole antenna size further. The working mechanism of the antenna miniaturization will be analyzed in the following part.

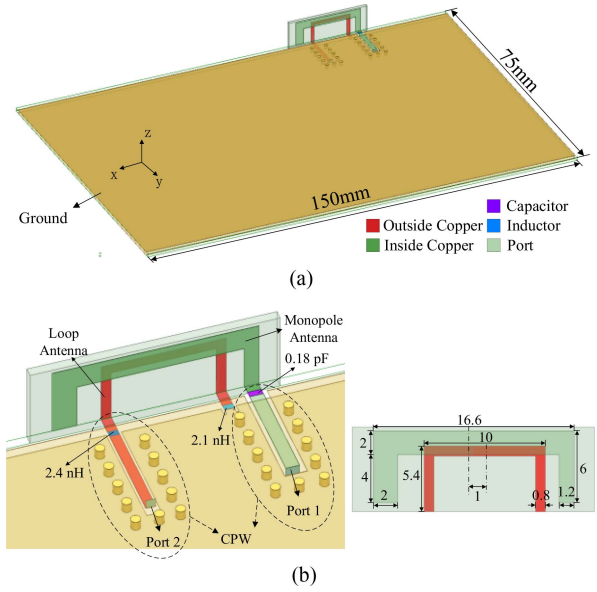

Fig. 2. Geometries of the first example with one capacitor loaded for the monopole antenna. (a) Antenna geometry. (b) Detailed view and dimensions. The unit used here is millimeters.

It is well known from the classical transmission line theory that a series lumped inductor could be equalized to a certain length of short-circuited transmission line [35]. Inspired by this concept, the loop antenna is loaded with two series inductors at the two ends, respectively, with one directly attached to the ground and another to the feeding port, as shown in Fig. 1(c). Since the boundary conditions at both ends of the loop antenna are still short-circuited, the proposed antenna is still a common-mode loop antenna. Thus, loading with a size-negligible lumped inductor can greatly reduce the antenna size. Similarly, a lumped capacitor can be introduced at the end of the monopole antenna to further reduce the size. Since the boundary condition is open-circuited, the current of the capacitor-loaded monopole antenna is still in-phase, presenting a quasi-differential-mode. Moreover, the lumped element on the feeding side also has the role of a series impedance matching element, especially for the large inductor and small capacitor, which can be used to further adjust the port impedance matching.

III. Demonstration Examples

Two demonstration examples are studied in this part. In the first example, there is only one capacitor loaded on the monopole antenna, while the second example involves two capacitors loaded on the monopole antenna.

A. First Example With Only One Capacitor Loaded

As shown in Fig. 2, a 0.18 pF lumped capacitor is connected in series at the feed-point of the monopole antenna. This implementation achieves miniaturization of the monopole antenna and facilitates matching adjustment. For the loop antenna, two inductors, one 2.4 nH and one 2.1 nH, are connected in series at its feed-point and ground-point, respectively. The substrate is FR4 with a relative permittivity of 4.2 and a loss tangent of 0.02. The monopole antenna is printed on the inner surface

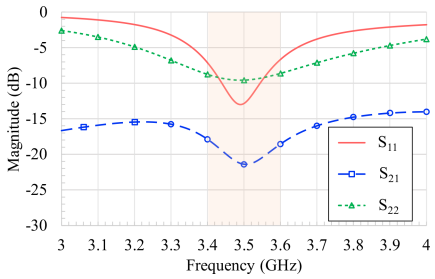

Fig. 3. Simulated *S*-parameters of the first example with only one capacitor loaded for the monopole antenna.

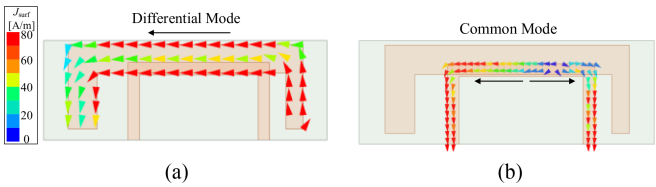

Fig. 4. Simulated current distributions of the first example. (a) Monopole antenna excited. (b) Loop antenna excited.

of the sideboard, while the loop antenna is patterned on its outer surface, and both antennas use the coplanar waveguide (CPW)-fed configuration, as illustrated in Fig. 2(a). During testing, coaxial feeding is employed, where the inner conductor is connected to the center strip and the outer conductor is attached to the coplanar ground planes. Therefore, the proposed antenna naturally avoids using balanced-feeding structures, so it is much easier for antenna integration. By adjusting the dimensions and relative position of the two antennas as well as the values of the lumped elements, there successfully appears a decoupling notch better than 20 dB at 3.5 GHz, as presented in Fig. 3, validating that the proposed antenna pair can realize self-decoupling with such asymmetric current distribution. One thing that should be mentioned is that a typical L-type or Π-type matching circuit can be designed at the two ports to further improve the impedance matching to be better than −10 dB, with the isolation almost unaffected.

The simulated current distributions of the antenna pair are depicted in Fig. 4 to investigate the decoupling principle. When port 1 is excited, the monopole antenna presents a quasi-differential mode. Differently, as the loop antenna is fed, the current null of the loop antenna is not at the center point but inclined toward the feeding side of the monopole antenna, which results from the fact that the two loaded inductors on the two ends of the loop antenna are unequal and the spatial couplings induced from the monopole antenna on the two half parts of the loop antenna are also asymmetric. Therefore, the mode orthogonality of the two antennas is eventually successfully constructed using the geometry asymmetry to compensate for the current asymmetry, so that an eventual self-decoupling is achieved.

B. Second Example With Two Capacitors Loaded

To further reduce the antenna size and improve the decoupling performance, another capacitor is loaded at the open end of the monopole antenna to achieve a more balanced differential mode,

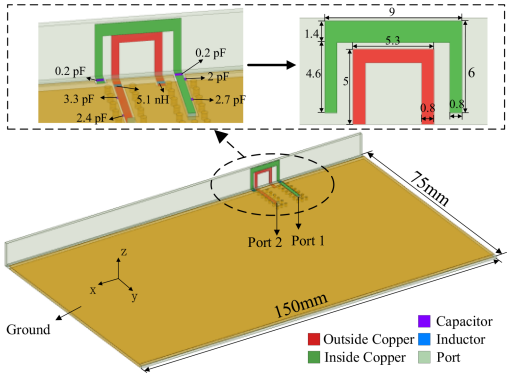

Fig. 5. Geometries of the second example with two capacitors loaded for the monopole antenna. The unit used here is millimeters.

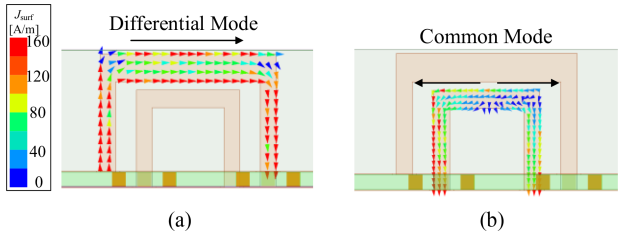

Fig. 6. Simulated current distribution of second example. (a) Port 1 excited. (b) Port 2 excited.

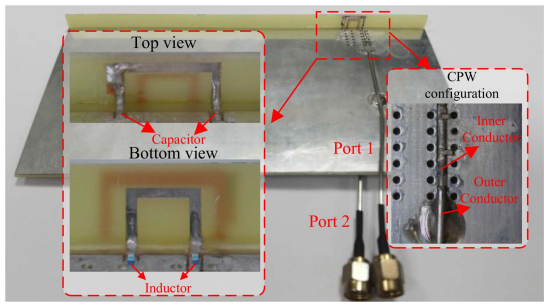

Fig. 7. Pictures of the fabricated prototype of the second example.

as illustrated in Fig. 5(a). Following the above analysis of the principal, the eventual design adopts two 0.2 pF capacitors on the monopole antenna ends and two 5.1 nH inductors on the loop antenna ends, with two matching circuits also introduced to enhance the impedance matching.

The simulated current distributions on the antenna pair excited at 3.5 GHz are described in Fig. 6. It can be seen from Fig. 6(a) that the modified monopole antenna generates a relatively balanced differential mode, exciting a symmetrical in-phase current when Port 1 is excited. On the contrary, as Port 2 is excited, the series of two identical inductors leads to a more balanced common mode, in which the current zero is located at the center of the loop antenna. Compared with the first example, the antenna size of the second example will be much smaller.

Fig. 7 shows a picture of the fabricated prototype of the second example, where the sideboard is enlarged to be seen in the red dashed square. The top view shows the monopole antenna, whose two ends are soldered to two capacitors. Similarly, the

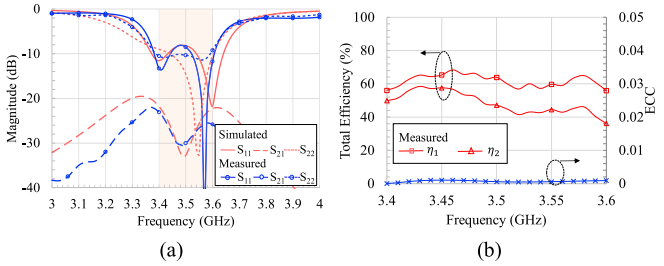

Fig. 8. *S*-parameters and radiation performance of the second example. (a) *S*-parameters. (b) Total efficiencies and ECC.

bottom view shows the inductor-loaded loop antenna. Besides, as shown in the right enlarged picture, the two antennas are fed by semi-rigid cables, whose inner conductor is soldered to the center strip of the CPW and the outer conductor to the coplanar ground. It can be observed from Fig. 8(a) that the measured *S*-parameters are consistent with the simulation results. The mutual coupling S_{21} is lower than -21.7 dB in the band from 3.4 GHz to 3.6 GHz, showing high isolation between the monopole antenna and the loop antenna. Moreover, the reflection coefficients S_{11} and S_{22} are both lower than -8 dB, benefiting from the lumped element loading at the feeding arms and the introduced matching elements.

To demonstrate the far-field radiation performance, the measured efficiencies and envelope correlation coefficients (ECCs) are depicted in Fig. 8(b). The measured average total efficiency of Port 1 is 61.7% while that of Port 2 is 48.4%. A higher efficiency can be expected for the loop antenna if two high-Q inductors are utilized. Besides, it is well known that the ECC is a key coefficient to evaluate the correlation performances of the MIMO antennas. In this study, the ECC is calculated using the measured far-field electric fields of the whole sphere. As also plotted in Fig. 8(b), the ECCs of the two antennas are lower than 0.002 within the operating band, showing a low spatial correlation for MIMO applications. In Fig. 9, the simulated and measured radiation patterns of the proposed MIMO antenna are depicted, where good agreement between them was achieved. Besides, a wide radiation coverage is observed for both antennas, guaranteeing the wide spatial coverage requirement of the terminal antennas.

A detailed comparison of the proposed antenna pair with several recent self-decoupled antenna pairs covering 3.4 GHz to 3.6 GHz is presented in Table I. It can be found that although the designs are free from using balanced feeding in [18], [19], and [29], the antenna size is somewhat bulky. On the other hand, while previous works [33], [34] based on orthogonality of the differential-mode antenna and the common-mode antenna can reduce the antenna size to some extent, both of them employ the 1/2λ antenna to excite the desired differential mode. Besides, most previous differential-mode antenna requires a balanced-feeding structure to excite the in-phase current. In contrast, in the proposed concept, the 1/4λ monopole antenna is utilized as a differential-mode antenna, and lumped elements are loaded to further minimize the antenna size, so the proposed antenna pair can possess a much smaller size compared to the previous designs with a comparable performance. Moreover, the utilization of the 1/4λ monopole antenna naturally avoids the requirement of balanced feeding, making it much easier for antenna integration in mobile terminals.

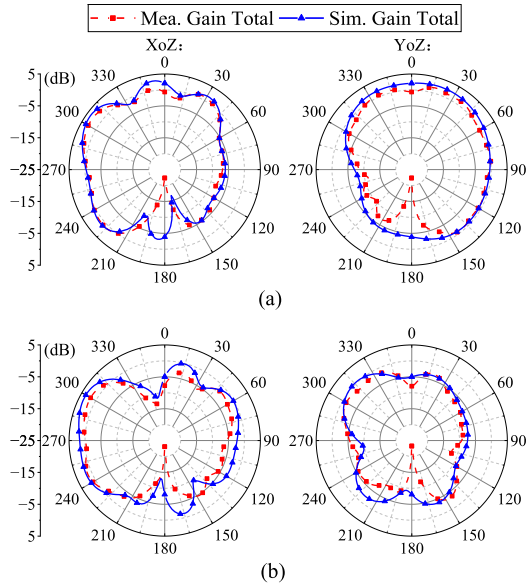

Fig. 9. Simulated and measured radiation patterns of the second example at 3.5 GHz. (a) Monopole antenna. (b) Loop antenna.

TABLE I
COMPARISON OF SEVERAL RECENT SELF-DECOUPLED ANTENNA PAIRS COVERING THE 3.4 GHZ TO 3.6 GHZ BAND

Ref.	Balanced feeding need	Aperture shared	Antenna Size(λ_0)	Isolation (dB)	Total Efficiency
[18][2024]	No	No	0.33	>17	>77% >67%
[19][2019]	No	No	0.23	>17	>60%
[29][2024]	No	Yes	0.7	>19.7	54-65%
[33][2020]	Yes	No	0.18	>20	52% 49%
[34][2023]	Yes	Yes	0.25	>24	>71%
Proposed	No	Yes	0.105	21.7	61.7% 48.4%

IV. CONCLUSION

In this letter, a 1/4λ monopole antenna is utilized as the differential-mode antenna to achieve an aperture-shared self-decoupled MIMO antenna design. The current distribution of the 1/4λ monopole antenna is in-phase but not symmetrical, so the antenna geometry and the arrangement are also deployed asymmetrically to compensate for the current nonsymmetry. Moreover, to further miniaturize the antenna size, lumped capacitors and inductors are loaded at the end of the monopole and loop antennas to replace the original long branches, and the working principle is well illustrated through a transmission-line model. Compared with the prior works, the proposed MIMO antenna does not require balanced-feeding structures, and the total antenna size is much smaller, with other performances comparable.

REFERENCES

[1] E. G. Larsson, O. Edfors, F. Tufvesson, and T. L. Marzetta, "Massive MIMO for next generation wireless systems," *IEEE Commun. Mag.*, vol. 52, no. 2, pp. 186–195, Feb. 2014.

[2] X. Chen, S. Zhang, and Q. Li, "A review of mutual coupling in MIMO systems," *IEEE Access*, vol. 6, pp. 24706–24719, 2018.

[3] Y. Wang and Z. Du, "A wideband printed dual-antenna with three neutralization lines for mobile terminals," *IEEE Trans. Antennas Propag.*, vol. 62, no. 3, pp. 1495–1500, Mar. 2014.

[4] S. Zhang and G. F. Pedersen, "Mutual coupling reduction for UWB MIMO antennas with a wideband neutralization line," *IEEE Antennas Wireless Propag. Lett.*, vol. 15, pp. 166–169, 2016.

[5] C.-D. Xue, X. Y. Zhang, Y. F. Cao, Z. Hou, and C. F. Ding, "MIMO antenna using hybrid electric and magnetic coupling for isolation enhancement," *IEEE Trans. Antennas Propag.*, vol. 65, no. 10, pp. 5162–5170, Oct. 2017.

[6] J. Deng, J. Li, L. Zhao, and L. Guo, "A dual-band inverted-F MIMO antenna with enhanced isolation for WLAN applications," *IEEE Antennas Wireless Propag. Lett.*, vol. 16, pp. 2270–2273, 2017.

[7] C.-Y. Chiu, C.-H. Cheng, R. D. Murch, and C. R. Rowell, "Reduction of mutual coupling between closely-packed antenna elements," *IEEE Trans. Antennas Propag.*, vol. 55, no. 6, pp. 1732–1738, Jun. 2007.

[8] B. K. Lau and J. B. Andersen, "Simple and efficient decoupling of compact arrays with parasitic scatterers," *IEEE Trans. Antennas Propag.*, vol. 60, no. 2, pp. 464–472, Feb. 2012.

[9] L. Zhao and K.-L. Wu, "A decoupling technique for four-element symmetric arrays with reactively loaded dummy elements," *IEEE Trans. Antennas Propag.*, vol. 62, no. 8, pp. 4416–4421, Aug. 2014.

[10] Y.-F. Cheng and K.-K. M. Cheng, "Compact wideband decoupling and matching network design for dual-antenna array," *IEEE Antennas Wireless Propag. Lett.*, vol. 19, no. 5, pp. 791–795, May 2020.

[11] W.-F. Zeng, F.-C. Chen, and Q.-X. Chu, "Bandwidth-enhanced 5G mobile phone antenna pair with tunable electric field null," *IEEE Trans. Antennas Propag.*, vol. 71, no. 2, pp. 1960–1964, Feb. 2023.

[12] L. Zhao, L. K. Yeung, and K.-L. Wu, "A coupled resonator decoupling network for two-element compact antenna arrays in mobile terminals," *IEEE Trans. Antennas Propag.*, vol. 62, no. 5, pp. 2767–2776, May 2014.

[13] M. Li, L. Jiang, and K. L. Yeung, "Novel and efficient parasitic decoupling network for closely coupled antennas," *IEEE Trans. Antennas Propag.*, vol. 67, no. 6, pp. 3574–3585, Jun. 2019.

[14] C. Deng, D. Liu, and X. Lv, "Tightly arranged four-element MIMO antennas for 5G mobile terminals," *IEEE Trans. Antennas Propag.*, vol. 67, no. 10, pp. 6353–6361, Oct. 2019.

[15] J. Sui and K.-L. Wu, "Self-curing decoupling technique for two inverted-F antennas with capacitive loads," *IEEE Trans. Antennas Propag.*, vol. 66, no. 3, pp. 1093–1101, Mar. 2018.

[16] J. Sui, C. Huang, and Y.-F. Cheng, "Multi-element fully-decoupled inverted-F antennas for mobile terminals," *IEEE Trans. Antennas Propag.*, vol. 70, no. 11, pp. 10076–10085, Nov. 2022.

[17] K.-L. Wong, C.-Y. Tsai, and J.-Y. Lu, "Two asymmetrically mirrored gap-coupled loop antennas as a compact building block for eight-antenna MIMO array in the future smartphone," *IEEE Trans. Antennas Propag.*, vol. 65, no. 4, pp. 1765–1778, Apr. 2017.

[18] H. Chen, D. He, M. Zhang, and Y. Dou, "Self-decoupled coupled line antenna pair (CLAP)," *IEEE Antennas Wireless Propag. Lett.*, vol. 23, no. 10, pp. 2944–2948, Oct. 2024.

[19] Z. Ren, A. Zhao, and S. Wu, "MIMO antenna with compact decoupled antenna pairs for 5G mobile terminals," *IEEE Antennas Wireless Propag. Lett.*, vol. 18, no. 7, pp. 1367–1371, Jul. 2019.

[20] Y.-F. Cheng and K.-K. M. Cheng, "Decoupling of two-element printed-dipole antenna array by optimal meandering design," *IEEE Trans. Antennas Propag.*, vol. 68, no. 11, pp. 7328–7338, Nov. 2020.

[21] J. Sui and K.-L. Wu, "A self-decoupled antenna array using inductive and capacitive couplings cancellation," *IEEE Trans. Antennas Propag.*, vol. 68, no. 7, pp. 5289–5296, Jul. 2020.

[22] X.-T. Yuan, Z. Chen, T. Gu, and T. Yuan, "A wideband PIFA-pair-based MIMO antenna for 5G smartphones," *IEEE Antennas Wireless Propag. Lett.*, vol. 20, no. 3, pp. 371–375, Mar. 2021.

[23] H. Li, Z. T. Miers, and B. K. Lau, "Design of orthogonal MIMO handset antennas based on characteristic mode manipulation at frequency bands below 1 GHz," *IEEE Trans. Antennas Propag.*, vol. 62, no. 5, pp. 2756–2766, May 2014.

[24] X. Zhao, S. P. Yeo, and L. C. Ong, "Decoupling of inverted-F antennas with high-order modes of ground plane for 5G mobile MIMO platform," *IEEE Trans. Antennas Propag.*, vol. 66, no. 9, pp. 4485–4495, Sep. 2018.

[25] Z. Wan, Y. He, Y. Bai, and H. Sun, "Miniaturized, low-profile, triple-band microstrip antenna and its four-antenna module for smartphone applications," *IEEE Trans. Antennas Propag.*, vol. 71, no. 12, pp. 9950–9955, Dec. 2023.

[26] L. Sun, Y. Li, Z. Zhang, and H. Wang, "Self-decoupled MIMO antenna pair with shared radiator for 5G smartphones," *IEEE Trans. Antennas Propag.*, vol. 68, no. 5, pp. 3423–3432, May 2020.

[27] B. Yang, Y. Xu, J. Tong, Y. Zhang, Y. Feng, and Y. Hu, "Tri-port antenna with shared radiator and self-decoupling characteristic for 5G smartphone application," *IEEE Trans. Antennas Propag.*, vol. 70, no. 6, pp. 4836–4841, Jun. 2022.

[28] A. Zhang, K. Wei, Y. Hu, and Q. Guan, "High-isolated coupling-grounded patch antenna pair with shared radiator for the application of 5G mobile terminals," *IEEE Trans. Antennas Propag.*, vol. 70, no. 9, pp. 7896–7904, Sep. 2022.

[29] Y. Fang, Y. Jia, J. Q. Zhu, Y. Liu, and J. An, "Self-decoupling, shared-aperture, eight-antenna MIMO array with MIMO-SAR reduction," *IEEE Trans. Antennas Propag.*, vol. 72, no. 2, pp. 1905–1910, Feb. 2024.

[30] L. Sun, H. Feng, Y. Li, and Z. Zhang, "Compact 5G MIMO mobile phone antennas with tightly arranged orthogonal-mode pairs," *IEEE Trans. Antennas Propag.*, vol. 66, no. 11, pp. 6364–6369, Nov. 2018.

[31] A. Ren, Y. Liu, and C.-Y.-D. Sim, "A compact building block with two shared-aperture antennas for eight-antenna MIMO array in metal-rimmed smartphone," *IEEE Trans. Antennas Propag.*, vol. 67, no. 10, pp. 6430–6438, Oct. 2019.

[32] H. Xu, S. S. Gao, H. Zhou, H. Wang, and Y. Cheng, "A highly integrated MIMO antenna unit: Differential/common mode design," *IEEE Trans. Antennas Propag.*, vol. 67, no. 11, pp. 6724–6734, Nov. 2019.

[33] L. Chang, Y. Yu, K. Wei, and H. Wang, "Orthogonally polarized dual antenna pair with high isolation and balanced high performance for 5G MIMO smartphone," *IEEE Trans. Antennas Propag.*, vol. 68, no. 5, pp. 3487–3495, May 2020.

[34] W. Hu et al., "Dual-band antenna pair with high isolation using multiple orthogonal modes for 5G smartphones," *IEEE Trans. Antennas Propag.*, vol. 71, no. 2, pp. 1949–1954, Feb. 2023.

[35] D. M. Pozar, *Microwave Engineering*. Hoboken, NJ, USA: Wiley, 2012, pp. 59–61.